Int. J. of Applied Mechanics and Engineering, 2006, vol.11, No.2, pp.245-254

dedicated to Professor K. Walters on his seventieh Birthday

TWO-DIMENSIONAL SIMULATIONS OF THE EFFECT OF THE RESERVOIR REGION ON THE PRESSURE OSCILLATIONS OBSERVED IN THE STICK-SLIP INSTABILITY REGIME

E. TALIADOROU and G. GEORGIOU*
Department of Mathematics and Statistics
University of Cyprus, P.O.BOX 20537, 1678 Nicosia, CYPRUS
e-mail: georgios@ucy.ac.cy

A. ALEXANDROU
Department of Mechanical and Manufacturing Engineering
University of Cyprus,
P.O.BOX 20537, 1678 Nicosia, CYPRUS

The time-dependent, two-dimensional compressible Newtonian flow over the reservoir-die region is solved assuming that slip occurs along the die wall following a nonmonotonic slip law. The combination of compressibility and nonlinear slip leads to self-sustained oscillations of the pressure drop and of the mass flow rate at constant piston speed, when the latter falls into the unstable negative slope regime of the flow curve. The effect of the reservoir volume on the amplitude, the frequency and the waveform of the pressure oscillations is studied and comparisons are made with experimental observations concerning the stick-slip polymer extrusion instability.

Key words: stick-slip instability, extrusion, compressibility, slip, pressure oscillations.

1. Introduction

Slip at the wall is considered to be a key factor in polymer extrusion instabilities, such as the stick-slip instability (Denn, 2001 and Hatzikiriakos and Migler, 2004). A characteristic of the stick-slip instability not encountered with other types of extrusion instability, such as sharkskin and gross melt fracture, is that this is accompanied by pressure and mass flow rate oscillations which result in extrudate shapes characterized by alternating rough and smooth regions (Denn, 2001 and Hatzikiriakos and Migler, 2004). Recent work concerning numerical modeling of the stick-slip instability has been reviewed by Achilleos ***et al.*** (2002) who discuss three different instability mechanisms: (a) combination of nonlinear slip with compressibility; (b) combination of nonlinear slip with elasticity; and (c) constitutive instabilities. In the present work, we investigate further the compressibility-slip instability by means of numerical simulations.

The compressibility-slip mechanism has been tested by Georgiou and Crochet (1994a; b) in the Newtonian case, with the use of an arbitrary nonmonotonic slip equation relating the wall shear stress to the slip velocity. These authors numerically solved the time-dependent compressible Newtonian Poiseuille and extrudate-swell flows with non-linear slip at the wall, showing that steady-state solutions in the negative-slope regime of the flow curve (i.e., the plot of the wall shear stress versus the apparent shear rate or the plot of the pressure drop versus the volumetric flow rate) are unstable, in agreement with linear stability analysis. Self-sustained oscillations of the pressure drop and of the mass flow rate at the exit are obtained, when an unstable steady-state solution is perturbed, while the volumetric flow rate at the inlet is kept constant. These oscillations are similar to those observed experimentally with the stick-slip extrusion instability. In a recent work,

* To whom correspondence should be addressed

Georgiou (2003) obtained similar results for the compressible, axisymmetric Poiseuille and extrudate-swell flows of a Carreau fluid with slip at the wall, using an empirical slip equation that is based on the experimental measurements of Hatzikiriakos and Dealy (1992a; b) on a HDPE melt. Unlike the experimental observations [see, e.g., Weill (1980), Hatzikiriakos and Dealy (1992b) and Durand *et al.* (1996)], however, the limit cycles of the periodic solution obtained in all these numerical studies do not follow the steady-state branches of the flow curve.

As stated in Georgiou (2003), including the reservoir is necessary in order to account for the compression and decompression of most part of the fluid, and obtain limit cycles following the steady-state branches of the flow curve, i.e., for obtaining pressure and extrudate flow rate oscillations characterized by abrupt changes, as in the experiments. Only such abrupt changes can lead to extrudates with alternating relatively smooth and sharkskin regions, which is the basic characteristic of the stick-slip instability. Note that the reservoir region is taken into account in various one-dimensional phenomenological models, which are also based on the compressibility/slip mechanism (Georgiou, 2004). These describe very well the pressure oscillations but they are not predictive, because they require as input certain experimental parameters.

The objective of the present work is to extend the simulations of Georgiou (2004) by including the reservoir region and study the effect of the reservoir length on the pressure oscillations. According to experiments (Myerholtz, 1967; Weill, 1980; Hatzikiriakos and Dealy, 1992b and Durand *et al.*, 1996), the period of the oscillations scales roughly with the volume of the polymer melt in the reservoir. Weill (1980) and Durand *et al.* (1996) also studied experimentally the effect of the reservoir length on the durations of compression and relaxation and found that both times increase linearly with the reservoir length, which indicates that the latter does not affect the waveform of the oscillations.

In Section 2, the governing equations, the slip equation and the boundary and initial conditions are discussed. In Section 3, we describe briefly the numerical method, present the numerical results, and make comparisons with experimental observations. Finally, in Section 4, we summarize the conclusions.

2. Governing equations and boundary conditions

The geometry of the flow corresponds to the actual setup used in the experiments of Hatzikiriakos and Dealy (1992b). There is a contraction region at *45* degrees between the barrel and the die as shown in Fig.1. The actual values of the radii of the barrel and the die, denoted respectively by R_b and R, and the length of the die, L, are tabulated in Tab.1. In the simulations, the length of the barrel, L_b, varied from *20R* to *200R*.

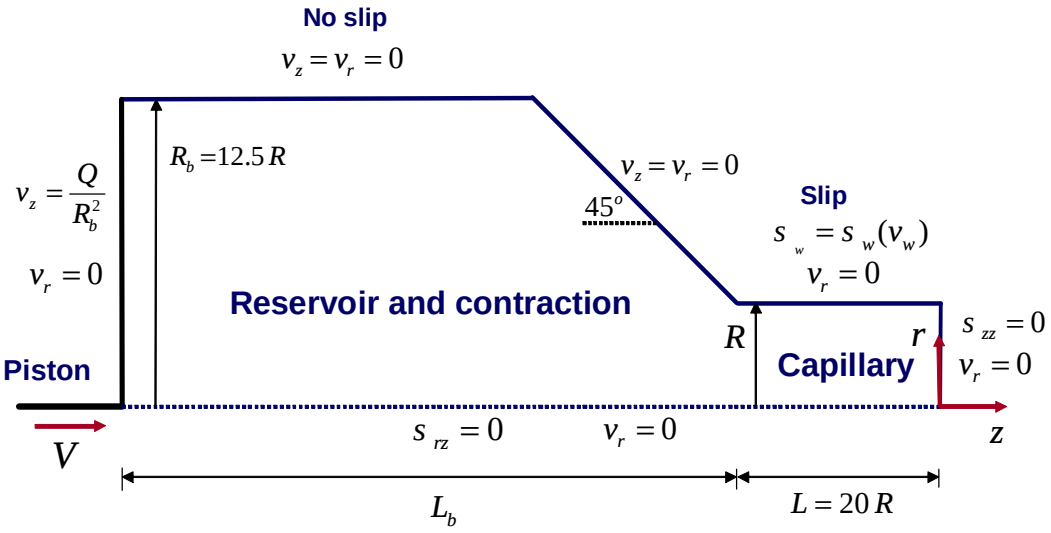

Fig.1. Geometry and boundary conditions for the time-dependent. compressible, axisymmetric flow over the reservoir-capillary region, with slip along the capillary wall.

Table 1. Symbols and values of various lengths concerning the flow geometry.

Symbol	Parameter	Value
R_b	Radius of the barrel	*0.9525 cm*
L_b	Length of the barrel	
	Contraction angle	*45 degrees*
R	Radius of the die	*0.0381 cm*
L	Length of the die	*0.762 cm*

To non-dimensionalize the governing equations, we scale the lengths by the capillary radius, R, the velocity vector, $\boldsymbol{v}$, by the mean velocity V in the capillary, the pressure, p, by $\eta V/R$, η denoting the constant viscosity, the density, ρ, by a reference density, ρ_0, and the time by R/V. With these scalings, the dimensionless continuity and momentum equations for time-dependent, compressible, isothermal viscous flow in the absence of body forces become

$$\frac{\partial \rho}{\partial t} + \nabla \cdot \rho \boldsymbol{v} = 0 , \tag{2.1}$$

and

$$\mathrm{Re}\,\rho\left(\frac{\partial \boldsymbol{v}}{\partial t} + \boldsymbol{v} \cdot \nabla \boldsymbol{v}\right) = -\nabla p + \nabla^2 \boldsymbol{v} \tag{2.2}$$

where Re is the Reynolds number, defined by

$$\mathrm{Re} \equiv \frac{\rho_0 R V}{\eta} . \tag{2.3}$$

The above equations are completed by an equation of state relating the pressure to the density. We used the first-order expansion

$$\rho = 1 + B\,p \tag{2.4}$$

where B is the compressibility number

$$B \equiv \frac{\beta \eta V}{R} , \tag{2.5}$$

β being the isothermal compressibility.

Along the capillary wall, slip is assumed to occur following the three-branch multi-valued slip model

$$\nu_w = \begin{cases} A_1 \sigma_w^{m_1}, & 0 \le \nu_w \le \nu_{c2} \\ A_2 \sigma_w^{m_2}, & \nu_{c2} \le \nu_w \le \nu_{min} \\ A_3 \sigma_w^{m_3}, & \nu_w \ge \nu_{min} \end{cases} \tag{2.6}$$

where ν_w is the relative dimensionless velocity of the fluid with respect to the wall, σ_w is the dimensionless shear stress on the wall, ν_{c2} is the maximum slip velocity at σ_{c2}, and ν_{min} is the minimum slip velocity at σ_{min}. The third branch is the power-law slip equation suggested by Hatzikiriakos and Dealy (1992b) for the right branch of their flow curve. The first branch results from the slip equation they propose for the left branch of their slope curve after substituting all parameters for resin A at $180^0 C$ and taking the normal stress as infinite. Finally, the second negative-slope branch, which corresponds to the unstable region of the flow curve for which no measurements have been possible, is just the line connecting the other two branches. The values of all the slip equation parameters and the definitions of the dimensionless numbers A_i can be found in Georgiou (2003).

The other boundary conditions of the flow are shown in Fig.1. Along the axis of symmetry, we have the usual symmetry conditions. Along the barrel and the contraction walls both velocity components are zero (no slip). Along the capillary wall, only the radial velocity is zero, whereas the axial velocity satisfies the slip Eq.(2.6). At the inlet plane, it is assumed that the radial velocity component is zero while the axial velocity is uniform, corresponding to the motion of the piston at constant speed. Note that the imposed volumetric flow rate, Q, is scaled by $\pi R^2 V$. The simulations are carried out on a fixed domain, i.e., the motion of the piston is not taken into account. This is a reasonable assumption provided that the piston speed is low. At the capillary exit, the radial velocity component and the total normal stress are assumed to be zero.

Finally, as the initial condition, we use the steady-state solution corresponding to a given volumetric flow rate Q_{old} that we perturb to Q at $t = 0$.

3. Numerical results

We use the finite element formulation for solving this Newtonian flow problem, employing biquadratic-velocity and bilinear-pressure elements. For the spatial discretization of the problem, we use the Galerkin forms of the continuity and momentum equations. For the time discretization, the standard fully-implicit (Euler backward-difference) scheme is used. Various finite element meshes have been used in the simulations with the reservoir length, L_b, ranging from *20* to *200*. These were refined near the walls, and around the entrance of the capillary. The longest mesh $(L_b = 200)$ consisted of *4511* elements corresponding to *42403* unknowns. In all results presented below the following values for the slip equation parameters and the compressibility number have been used: $m_1 = 3.23$, $A_1 = 0.0583$, $m_2 = 2.86$, $A_2 = 0.929$, $m_3 = -4.43$, $A_3 = 4.04$ and $b = 1.54\,10^{-4}$.

We first constructed the steady-state flow curves for the reservoir-capillary region. In Fig.2, we show the log-log plot of the pressure drop, measured along the centerline from the piston to the die exit, versus the volumetric flow rate obtained with $\mathrm{Re} = 0.01$ and $L_b = 80$. Due the nonmonotonicity of the slip equation, the flow curve exhibits a maximum and a minimum, which define the limits of the unstable regime, i.e., only the steady-state solutions corresponding to the two positive-slope branches are stable. As already mentioned, the steady-state solutions are perturbed by changing the volumetric flow rate from an old value to the desired one

Q. Given that the flow is compressible, the behavior of the time-dependent solution depends on whether the new value of *Q* corresponds to a positive-slope branch, or to the negative-slope branch which is unstable. In the first case, the new steady-state is obtained without any oscillations, whereas, in the second case, the solution is oscillatory and, after a transition period, becomes periodic. Self-sustained oscillations of the pressure drop and the mass flow rate are obtained which are similar to those observed experimentally in the stick-slip extrusion instability regime. All the results presented below have been obtained in the unstable regime.

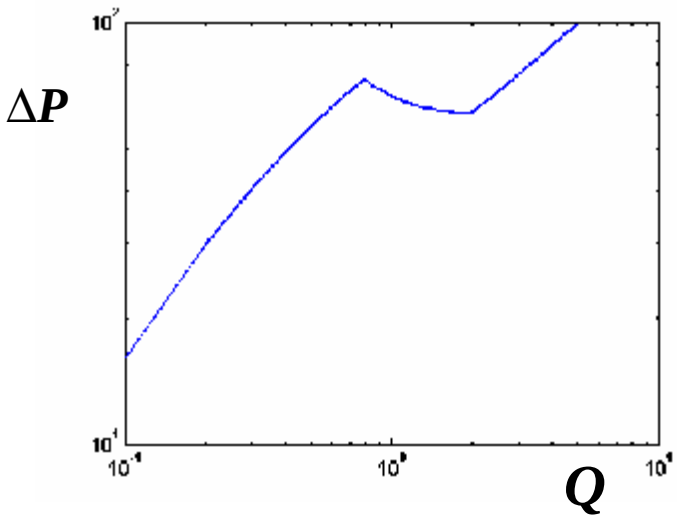

Fig.2. Flow curve for Re=*0.01* and $L_b = 80$.

In Fig.3, we show the oscillations of the pressure drop and the volumetric flow rate obtained by perturbing the steady-state solution for $\mathrm{Re} = 0.01$, $L_b = 80$ and $Q = 1.35$. In Fig.3a, we show two different possibilities when the pressure drop is measured across the entire flow domain, $(\Delta P)_{tot}$ and across the capillary, $(\Delta P)_{cap}$. Sudden jumps of the pressure drop are observed in the latter case. The volumetric flow rate at the capillary exit is also characterized by sudden jumps which is consistent with experimental observations. Plotting the trajectory of the solution on the flow curve plane (Fig.4) shows that, after a transition period, a limit cycle is reached which follows exactly the positive-slope branches of the steady-state flow curve. The volumetric flow rate increases together with the pressure following exactly the left positive-slope branch of the flow curve and, when the pressure reaches its maximum value, *Q* jumps to the right positive slope branch. The volumetric flow rate then starts decreasing together with the pressure following this branch till the pressure reaches its minimum and then jumps to the left positive-slope branch and starts the next oscillation cycle. This behavior agrees well with experimental observations (Hatzikiriakos and Dealy, 1992b and Durand *et al.*, 1996). Note also that in our previous study (Georgiou, 2003), the limit cycles did not follow the steady-state flow curve due to the omission of the reservoir region. This drawback was also exhibited by the one-dimensional model of Greenberg and Demay (1994), which does not include the barrel region. Note that one-dimensional phenomenological relaxation/oscillation describe the oscillations of the pressure and the volumetric flow rate in the stick-slip instability regime under the assumption that these follow the experimental flow curve [see Adewale and Leonov (1997) and Den Doelder *et al*. (1998) and references therein]. The present simulations are the first to show that the limit cycle follows the steady-state flow curve.

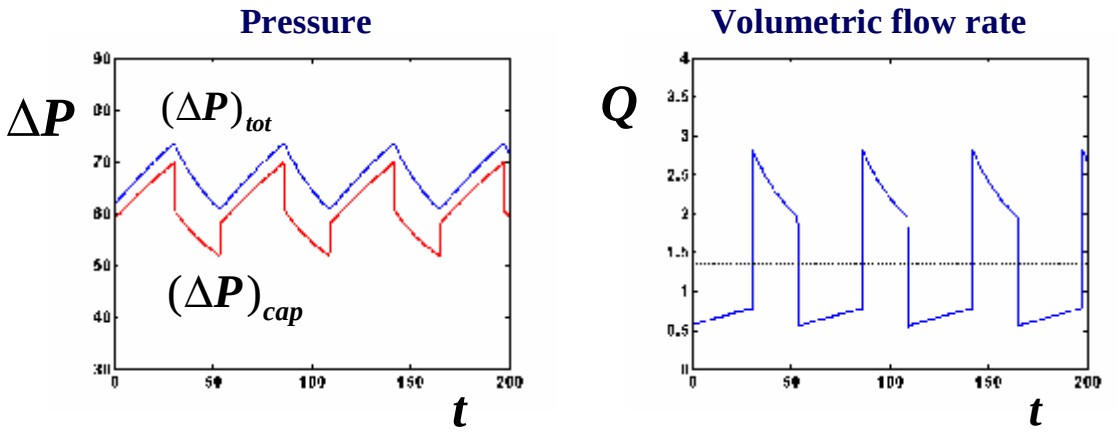

Fig.3. Pressure and flow rate oscillations for $Q=1.35$, Re=0.01 and $L_b = 80$.

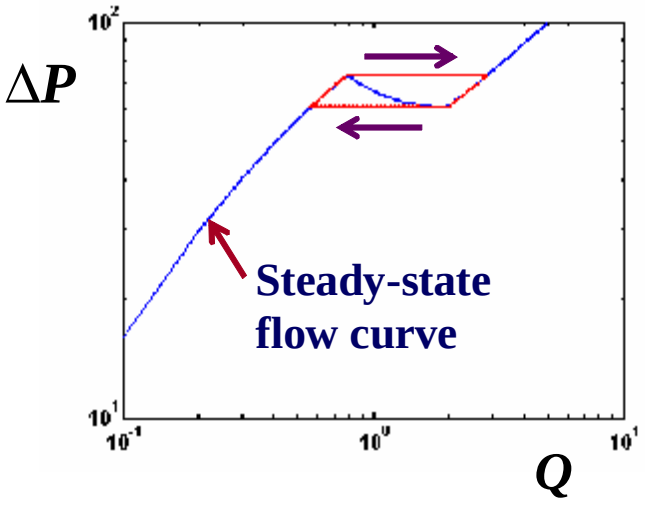

Fig.4. Trajectory of the solution on the flow curve plane; $Q=1.35$, Re=0.01 and $L_b = 80$.

We then reduced the value of the Re from 0.01 to 0.001 in an attempt to approach the experimental value $\left(1.43 \cdot 10^{-5}\right)$. As shown in Fig.5, where we compare the oscillations of ΔP during one cycle for $\mathrm{Re} = 0.01$ and 0.001, $L_b = 80$ and $Q = 1.35$, decreasing the Reynolds number has no practical effect on the oscillations. However, the artificial overshoots are observed in the flow rate. Thus instead of trying to eliminate the overshoots by reducing the time step (which would have resulted in much longer runs), we decided to continue the runs with $\mathrm{Re} = 0.01$. Note that in our previous study (Georgiou, 2003) for the extrudate-swell flow, in which the reservoir region has been excluded, we observed that as the Reynolds number is reduced the amplitude of the pressure-drop oscillations is reduced, the amplitude of the mass-flow-rate oscillations is increased and the frequency of the oscillations is considerably increased. This shows once again the importance of including the reservoir region.

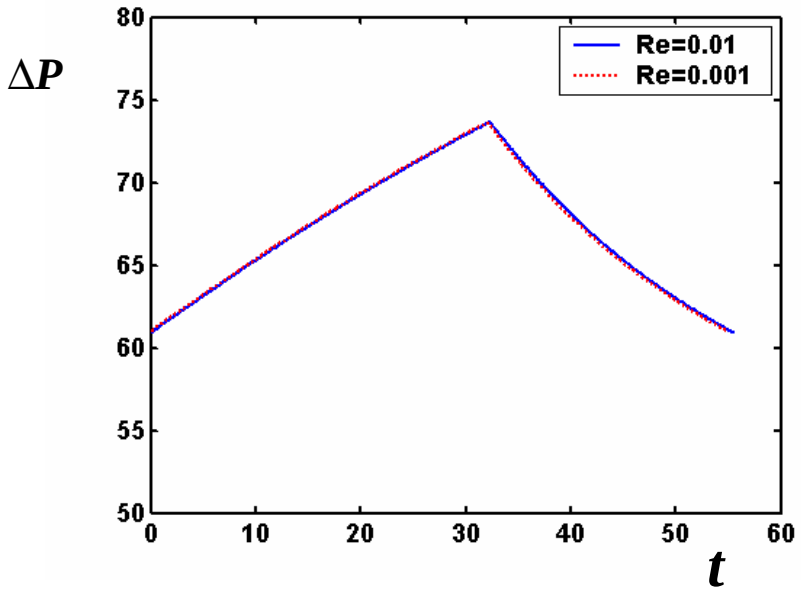

Fig.5. Comparison of the pressure oscillations for Re=*0.01* and *0.001*; $L_b = 80$ and *Q=1.35.*

In order to study the effect of the reservoir length on the pressure oscillations we obtained results for various values of L_b. In Fig.6, we show the pressure oscillations for different values of L_b, Re $= 0.01$ and *Q=1.35*. We observe that the period of the pressure oscillations increases with L_b while their amplitude seems to be less sensitive. This is more clearly shown in Fig.7, where the period and the amplitude of the pressure oscillations are plotted versus the reservoir volume. In agreement with experiments (Hatzikiriakos and Dealy, 1992b; Durand *et al.*, 1996; Sato and Toda, 2001 and Robert *et al.*, 2001), the period *T* increases linearly with the reservoir volume while the amplitude is essentially constant. In Fig.7a, the period appears to pass through the origin which is not the case with the experiments. Finally, in order to show the effect of the reservoir on the waveform of the pressure oscillations we plotted the normalized pressure oscillations during one cycle for $L_b = 20$ and *200* (Fig.8). The waveform is independent of the reservoir length, i.e., the durations of the compression and relaxation increase linearly with the reservoir length. This agrees well with the experiments of Weill (1980), Hatzikiriakos and Dealy (1992b) and Durand *et al.* (1996).

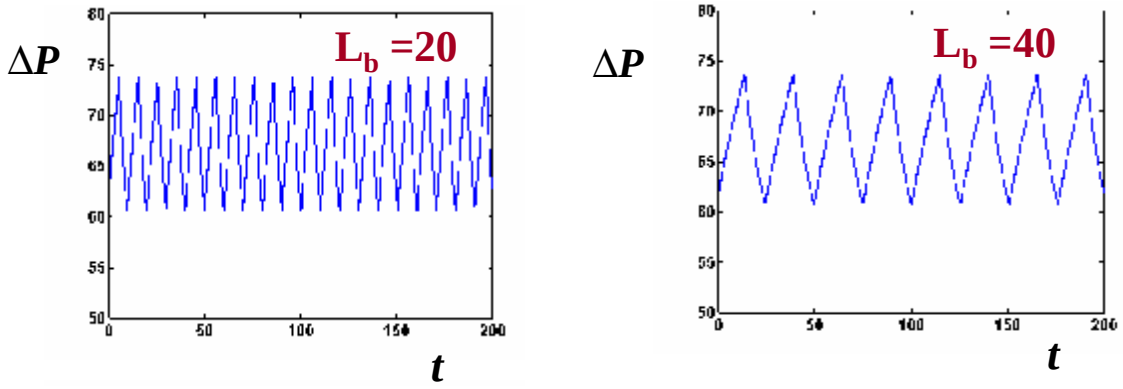

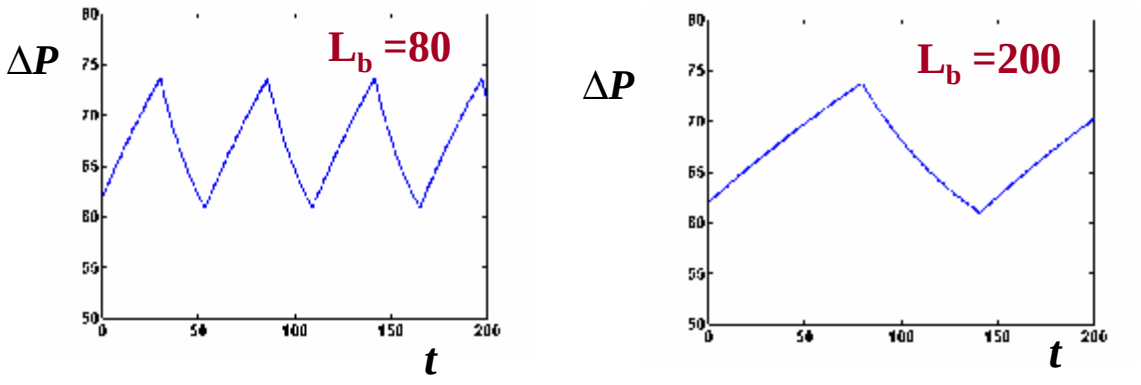

Fig.6. Effect of the reservoir length on the pressure oscillations; *Q=1.35* and Re=*0.01*.

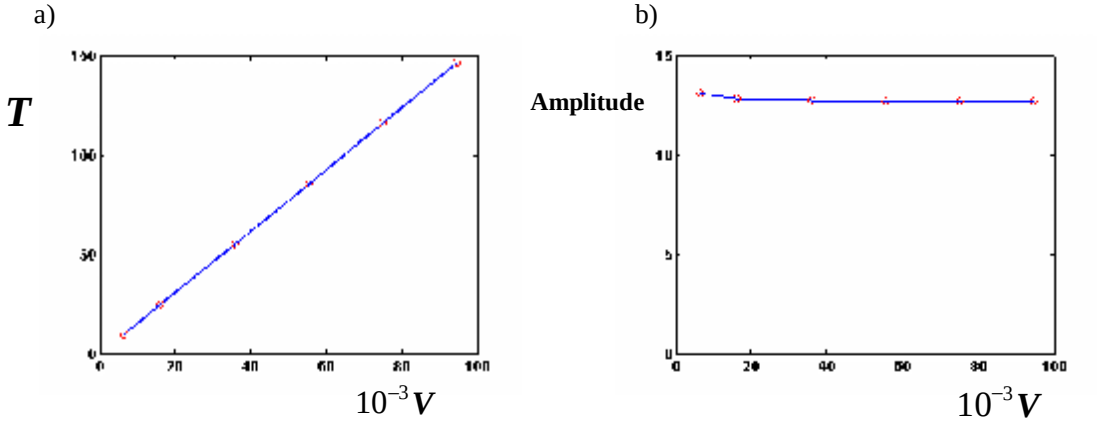

Fig.7. The period and the amplitude of the pressure oscillations versus the reservoir volume; *Q=1.35* and Re=*0.01*.

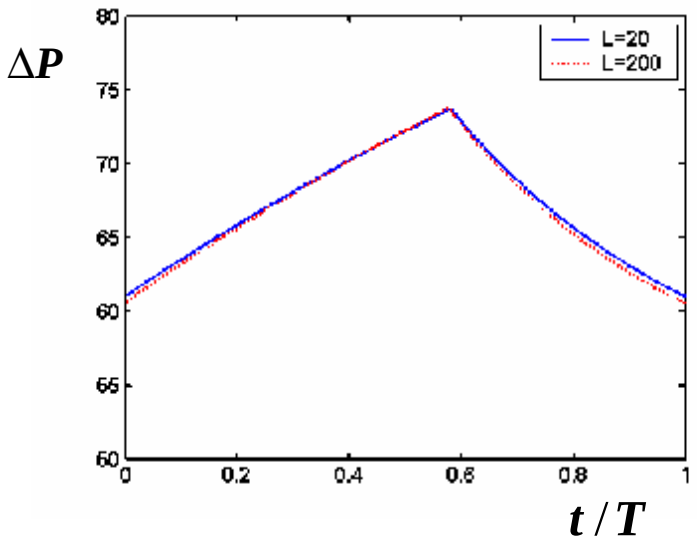

Fig.8. Effect of the reservoir length on the waveform of the pressure oscillations; *Q=1.35* and Re=*0.01*.

4. Conclusions

We solved numerically the time-dependent, compressible flow of a Newtonian fluid over the reservoir-capillary region, assuming that slip occurs along the capillary wall following a nonmonotonic slip law based on the experimental findings of Hatzikiriakos and Dealy (1992a; b) for certain polyethylene melts. By using meshes of different length, we have studied the effect of the reservoir length on the pressure oscillations occurring when the imposed flow rate falls in the unstable negative-slope regime of the flow curve. Our calculations showed that the pressure oscillations follow the steady-state flow curve and that their period increases linearly with the reservoir length, while their amplitude and waveform remain unaffected. These results are in good agreement with the experiments of Weill (1980), Hatzikiriakos and Dealy (1992b), Durand *et al*. (1996), and others, which have also shown that the period and the shape of the pressure oscillations vary also with the imposed flow rate, whereas their amplitude remains unaffected. The effect of Q on the pressure oscillations is currently under study.

References

Achilleos E., Georgiou G. and Hatzikiriakos S.G. (2002): *On numerical simulations of polymer extrusion instabilities*. –Applied Rheology, vol.12, pp.88-104.

Adewale K.P. and Leonov A.I. (1997): *Modelling spurt and stress oscillations in flows of molten polymers*. – Rheol. Acta., vol.36, pp.110-127.

Denn M.M. (2001): *Extrusion instabilities and wall slip*. – Annu. Rev. Fluid Mech., vol.33, pp.265-287.

Den Doelder C.F.J., Koopmans R.J., Molenaar J. and Van de Ven A.A.F. (1998): *Comparing the wall slip and the constitutive approach for modelling spurt instabilities in polymer melt flows*. – J. Non-Newtonian Fluid Mech., vol.75, pp.25-41.

Durand V., Vergnes B., Agassant J.F., Benoit E. and Koopmans R.J. (1996): *Experimental study and modeling of oscillating flow of high density polyethylenes*. – J. Rheology, vol.40, pp.383-394.

Georgiou G.C. and Crochet M.J. (1994a): *Compressible viscous flow in slits with slip at the wall*. – J. Rheol., vol.38, pp.639-654.

Georgiou G.C. and Crochet M.J. (1994b): *Time-dependent compressible extrudate-swell problem with slip at the wall*. – J. Rheol., vol.38, pp.1745-1755.

Georgiou G. (2003): *The time-dependent compressible Poiseuille and extrudate-swell flows of a Carreau fluid with slip at the wall*. – J. Non-Newtonian Fluid Mech., vol.109, pp.93-114.

Georgiou G. (2004): *Stick-slip instability*. In: Polymer Processing Instabilities: Control and Understanding, S.G. Hatzikiriakos and K. Migler (Eds.). – New York: Mercel Dekker.

Greenberg J.M. and Demay Y. (1994): *A simple model of the melt fracture instability*. – Eur. J. Appl. Maths., vol.5, pp.337-357.

Hatzikiriakos S.G. and Dealy J.M. (1992a): *Wall slip of molten high density polyethylenes. II. Capillary rheometer studies*. – J. Rheol., vol.36, pp.703-741.

Hatzikiriakos S.G. and Dealy J.M. (1992b): *Role of slip and fracture in the oscillating flow of HDPE in a capillary*. – J. Rheol., vol.36, pp.845-884.

Hatzikiriakos S.G. and Migler K. (2004): *Polymer Processing Instabilities: Control and Understanding*. – New York: Mercel Dekker.

Myerholtz R.W. (1967): *Oscillating flow behavior of high-density polyethylene melts*. – J. Appl. Polym. Sci., vol.11, pp.687-698.

Robert L., Vergnes B. and Demay Y. (2001): *Complex transients in the capillary flow of linear polyethylene*. – J. Rheol., vol.44, pp.1183-1187.

Sato K. and Toda A. (2001): *Physical mechanism of stick-slip behavior in polymer melt extrusion: Temperature dependence of flow curve*. – J. Phys. Soc. Japan, vol.70, pp.3268-3273.

Weill A. (1980): *Capillary flow of linear polyethylene melt: Sudden increase of flow rate*. – J. Non-Newtonian Fluid Mech., vol.7, pp.303-314.

Received: February 8, 2005